STABILITY OF SHELLS IN THE CONDITIONS
OF PLASTIC FLOW OF MATERIAL

JAKUB MARCINOWSKI

Institute of Structural Engineering, University of Zielona Góra,
Szafrana 2, 65-516 Zielona Góra, Poland.

PIOTR KONDERLA, KATARZYNA DOMARADZKA*

Institute of Civil Engineering, Wrocław University of Technology,
Wybrzeże Wyspiańskiego 27, 50-370 Wrocław, Poland.

Abstract: The paper outlines a procedure for performing the numerical analysis of the stability of steel cylindrical shell structure. The system COSMOS/M based on FEM was employed. The analysis was carried out in both geometrically and physically nonlinear ranges. Several methods of controlling equilibrium path parameter were tested.

Streszczenie: Przedstawiono analizę numeryczną dotyczącą stateczności stalowej powłoki walcowej. W analizie wykorzystano system COSMOS/M oparty na MES.W obliczeniach uwzględniono nieliniowe efekty geometryczne i fizyczne. Przetestowano liczne sposoby sterowania parametrem ścieżki równowagi.

Резюме: Представлен численный анализ, касающийся устойчивости стальной цилиндрической
оболочки. В анализе использована система COSMOS/M, базирующая на MES. В расчетах учтены нелинейные геометрические и физические эффекты. Протестированы многочисленные способы управления параметром дорожки равновесия.

1. INTRODUCTION

In this paper, the results of the numerical analysis of stability of a cylindrical shell under transverse load are considered. In the analysis, the Finite Elements Method was used. Numerical tests were carried out using COSMOS/M software.

The solution of the problem relies on determining nonlinear equilibrium path of an elastic-plastic shell in the load-displacement space [6]. The equilibrium path is formed by several points which are determined using the incremental-iterative Raphson–Newton method [1]. The iteration is shown in figure 1. The iteration formula of the NR method for the *i*-th increment is given by:

$$\mathbf{K}_T^m \cdot \Delta \mathbf{u}^{m+1} = P^{i+1} - F^m .$$ (1)

---

* To whom correspondence should be addressed.

In every iteration step, the tangent stiffness matrix $\mathbf{K}_T^m$ is generated and equilibrium of the system is verified. The residual quantities F^m occurring in equation (1) are defined in figure 1. The parameter λ represents the load intensity and P_0 is the reference load. Only quasi-static, one-parameter loads were considered.

The efficiency and speed of this method may be improved by using the option of automatic selection of incremental steps, which was applied in the example presented. It has been shown that of all the methods this one is most effective.
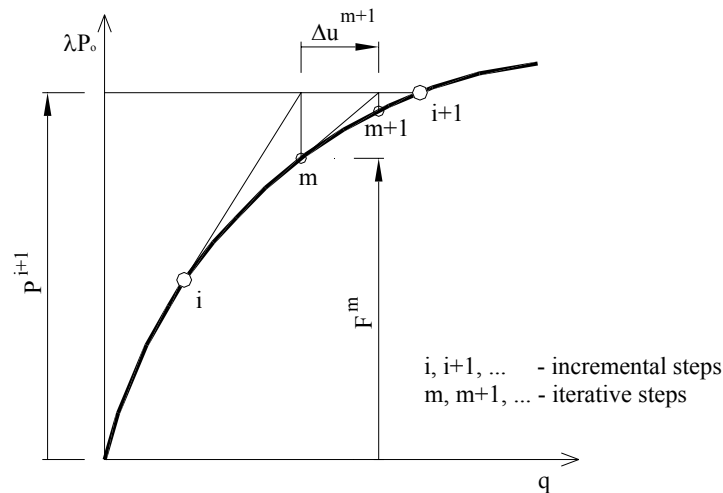

Fig. 1. Scheme of iterative technique in an incremental step of the Newton–Raphson method

While determining the equilibrium paths in the load–displacement configuration both pre-critical and post-crtitical states were observed. The shell analysed revealed a snap-through behaviour [2] (figure 2).

The characteristic points on the equilibrium path are the critical points corresponding to the critical states of the construction. Our considerations were confined to the limit points on the fundamental equilibrium path – the upper and lower limit points, marked as PG1 and PG2. In real construction, exhibiting the equilibrium path of this type, in an initial phase of load the path is stable; in PG1, the system loses its stability and then the dynamical snap-through to the position 1 (figure 2) occurs. The unloading runs on the part of the path from the point 1 to the point PG2 where the snap-back takes place. Unstable equilibrium states occurring on the path beetween the points PG1 and PG2 cannot be reached by controlling load parameter, therefore in the research a displacement control was applied. It is also possible to control calculations by the parameter of the arc.
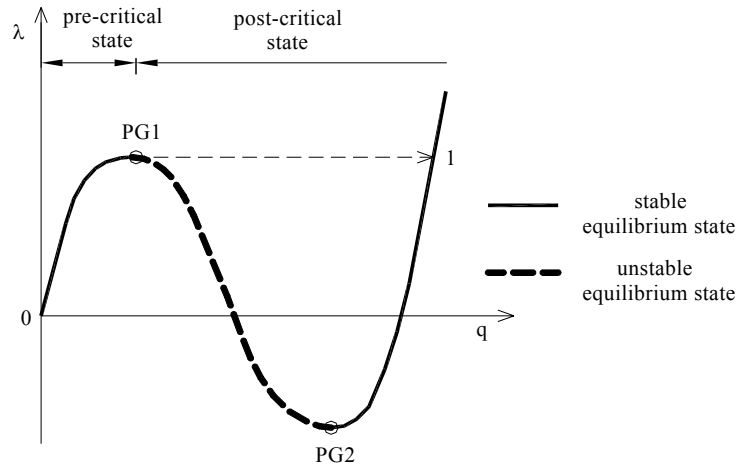
Fig. 2. Equilibrium states on the load–displacement path

2. NUMERICAL ANALYSIS EXAMPLE

A steel cylindrical shell, being the subject of the analysis, is simply supported along its rectilinear edges. Curvilinear edges are free. Load of the shell of the intensity *q* was applied as uniformly distributed, placed along rectilinear symmetry axis. Geometry, the method of supporting, the way of distribution of the load and the finite elements mesh used in computations are shown in figure 3.

h = 5 mm, f = 10 mm, L = 400 mm, b = 420 mm;
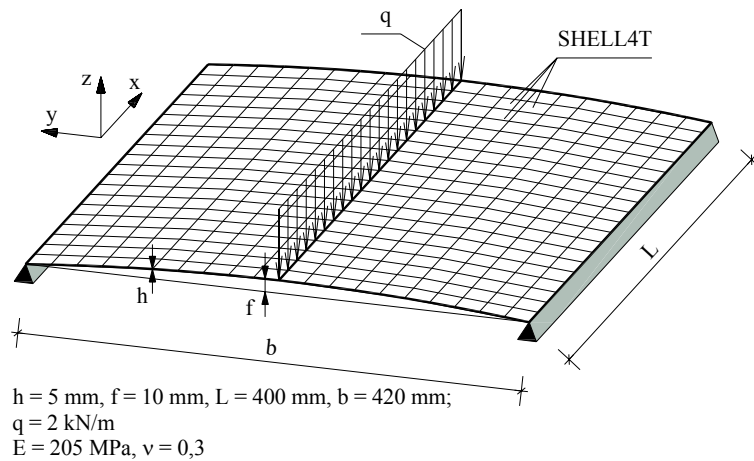q = 2 kN/m
E = 205 MPa, ν = 0,3

Fig. 3. Static scheme and discrete model of the shell structure analysed

In the discrete FEM model, SHELL4T elements were used. The shell was divided into 400 quadrilateral, 4-node finite elements. Every node has six degrees of freedom (three displacements and three rotations). This element is used for modelling thick shells and thermally loaded structures [7]. In the present analysis, an isotropic material was used.

The parameters of the material corresponding to St3S steel were accepted. The elastic-plastic model of material with isotropic strain hardening was used, where the tangent module value E_T is equivalent to 0.001 of Young's modulus value E (E = 205 MPa, E_T = 205 kPa). Moreover, the Huber–Mises–Hencky plasticity condition was exploited [7], in which the surface of plasticity is given by

$$F(\sigma_{ij}) = \sqrt{3}\,\bar{\sigma} - \sigma_y = 0, \tag{2}$$

where σ_y is the yield stress, whereas the reduced stress is equal to:

$$\bar{\sigma} = \sqrt{\frac{1}{2}(|\sigma_1 - \sigma_2|^2 + |\sigma_2 - \sigma_3|^2 + |\sigma_1 - \sigma_3|^2)}. \tag{3}$$

Comparative numerical analysis for three variants of shell – the shell of the same geometry and load, but different material properties – was done. The equilibrium paths for the materials of yield stresses appropriately R_e = 235 MPa (variant 1), R_e = 300 MPa (variant 2) and R_e = 600 MPa (variant 3) were calculated. Real value of yield stress was increased to the value allowing the elastic behaviour of the shell in pre-critical range to be reached. In this particular case, only geometrical nonlinearity affects the analysis results.

After many trials of implementing different methods for solving the nonlinear problem, the iterative Newton–Raphson technique with displacement parameter control was chosen. The controlling parameter was the rotation of the 115th node, (marked in figure 4 as node A), about the x-axis. The node localization chosen ensures that in the path a rotation angle does not change its sign.

The step of a constant increment in the angle displacement was accepted in variants 1 and 2. Time curve was defined – final time value is equivalent to angle displacement of 0.2 radian.

Figure 4 demonstrates the results of numerical analysis in the form of the projection of equilibrium paths onto load–displacement space. The equilibrium paths in a central node were compared successively for three values of the yield stress. All of the three paths exhibit limit points and one of them also the turning point. The coordinates of the point PG1 change concurrently with a yield stress increase.

The point PG2 was reached only in variants 1 and 2. In variant 3 close by the expected point PG2, a divergence of algorithm based on displacement control was observed. Such a shape of equilibrium path suggested the existence of turning point on the path; unfortunately, divergence could not be prevented despite changing the displacement control parameter to arc-length parameter.
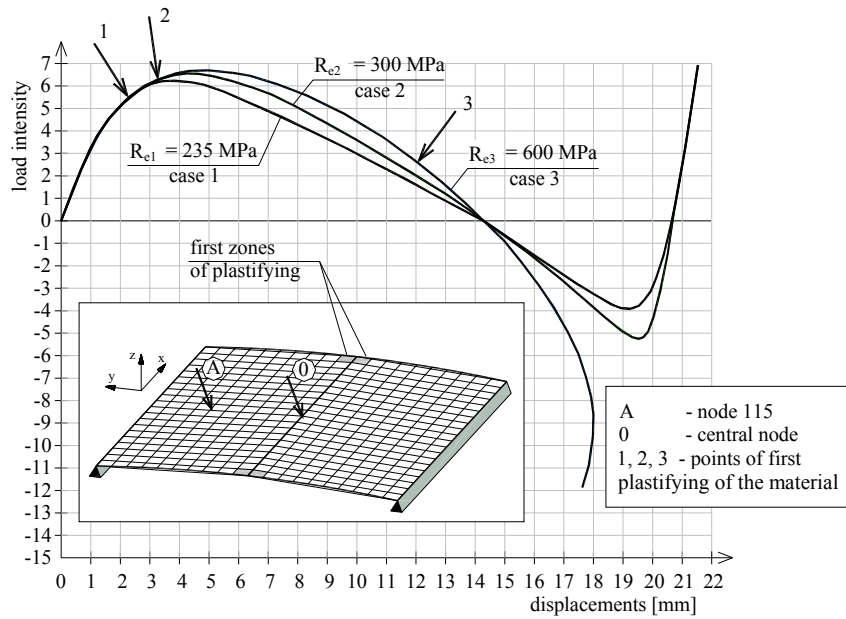
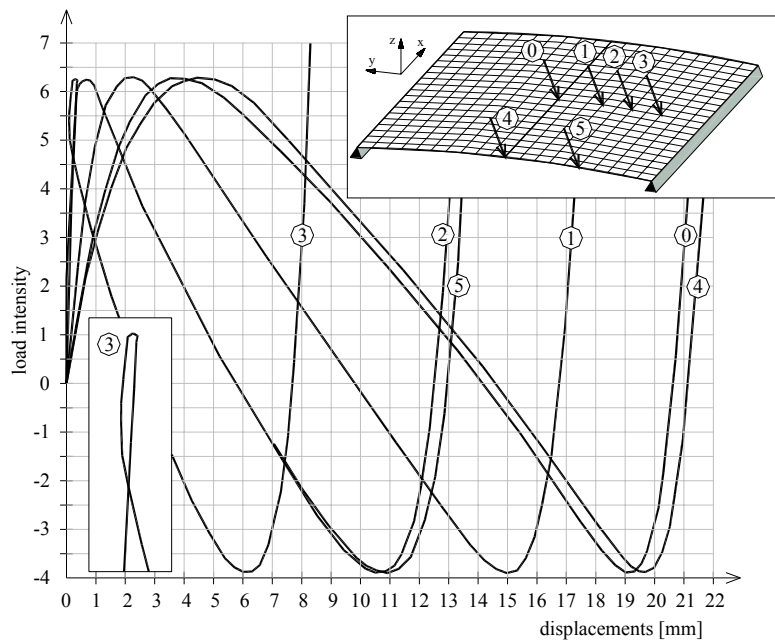Fig. 4. Comparison of equilibrium paths at different values of R_e

Fig. 5. Comparison of equilibrium paths for several nodes (case no. 1)

It is interesting that the equilibrium paths have common point on the level of $\lambda = 0$, which does mean that the yield stress value has no influence on the displacement at this particular load intensity. Moreover, no differences due to different values of R_e in post-critical range were observed. Apparently the snap through follows unload and return to an elastic range. The cases analysed were also compared in terms of plasticity zones expansion. And so, a plastic stress occurs for the first time in the central node and is responsible for the displacement of about 2.5 mm in the case 1, about 3.5 mm in the case 2, and about 12 mm in the case 3 only in unstable configuration.

The expansion of plasticity zone has its origin in terminal elements marked in figure 4, and then gradually covers four central strips of finite elements.

Comparative analysis of equilibrium paths in different nodes of the shell was also carried out. Figure 5 shows the paths for the nodes on the y-axis of the shell and for the nodes on a free edge. Our analysis is carried out at $R_e = 235$ MPa. These paths represent the succession of deformation of the shell in consecutive points of the path. The paths demonstrated are in fact the projections of the calculated equilibrium path onto consecutive load–displacement subspaces.

In the neighbourhood of the first limit point, for nodes localized nearby support, a loop is forming, and this detail is precisely shown by a separated fragment of figure 5. This does mean that in this range of load intensity change, this zone is shortly elevated.

Maximum displacement achieved during numerical analysis was revealed in central nodes localized on unbounded edges and its value approached 25 mm. Figure 6 illustrates the state of stress (equation (3)) in several points on the equilibrium path for elastic-plastic solution. These graphs refer to top surface and are shown in deformed configurations.

a)   b)

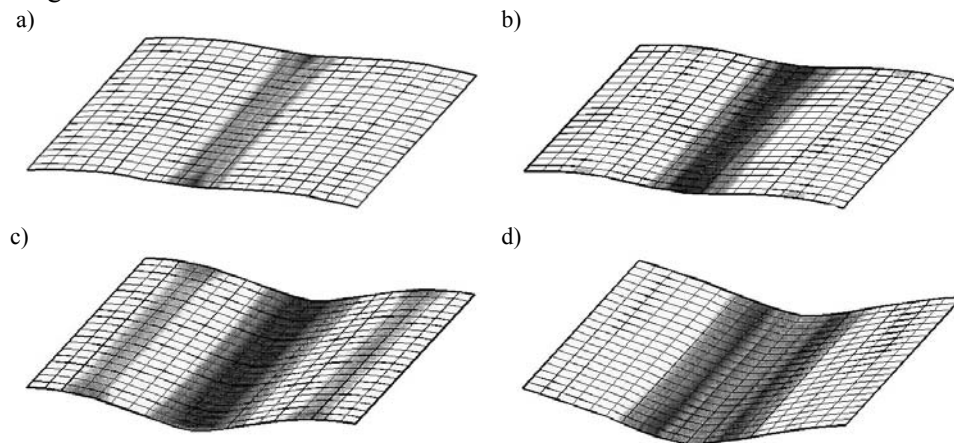c)   d)

Fig. 6. Expansion of plastic zone in several points on equilibrium path (case no. 1):
a) the first plastic stress, b) the limit point (PG1), c) at $\lambda = 0$, d) the limit point (PG2)

3. CONCLUSIONS

The comparative analysis of the stability of shells made it possible to estimate the influence of several factors on construction behaviour in both geometrically and physically nonlinear ranges. The influence of yield stress on the localization of limit points on the equilibrium path and on plastic zone expansion in the shell was investigated. The displacement values in several nodes of the shell were compared.

Several algorithms for equilibrium path calculation were tested. The Newton–Raphson method with displacement control proved to be most effective.

The aim of the study was to analyse the phenomena of stability loss of the shell of certain dimensions made of material revealing particular plastic features. The results obtained in numerical tests will allow the design of the stand for experimental investigation of the stability of steel cylindrical shells.

REFERENCES

[1] CICHOŃ Cz., *Nieliniowa analiza stateczności konstrukcji prętowych w ujęciu MES*, Wydawnictwo Politechniki Krakowskiej, Monografia, 38, 1985.
[2] MARCINOWSKI J., *Nieliniowa stateczność powłok sprężystych*, Oficyna Wydawnicza Politechniki Wrocławskiej, 1999.
[3] ROORDA J., *Problemy stateczności konstrukcji sprężystych*, *Wybrane zagadnienia stateczności konstrukcji*, Ossolineum, 1981.
[4] RUSIŃSKI E., *Metoda elementów skończonych, System Cosmos/M*, Wydawnictwa Komunikacji i Łączności, Warszawa, 1994.
[5] WASZCZYSZYN Z., CICHOŃ Cz., *Metody rozwiązywania nieliniowych zagadnień statyki i stateczności konstrukcji w ujęciu MES. Wybrane zagadnienia stateczności konstrukcji*, Ossolineum, 1987.
[6] WASZCZYSZYN Z., CICHOŃ Cz., RADWAŃSKA M., *Metoda elementów skończonych w stateczności konstrukcji*, Wydawnictwo Arkady, Warszawa, 1990.
[7] COSMOS/M 2.5 Electronic documentation.